

## Appendix A.

### Supplementary data.

#### Synthesis and structure of annulated dithieno[2,3-*b*;3',2'-*d*]thienyl- and ring-opened 3,3'-bithienyl Fischer carbene complexes

Zandria Lamprecht,<sup>a</sup> Frederick P. Malan,<sup>a</sup> David C. Liles,<sup>a</sup> Simon Lotz<sup>a</sup> and Daniela I. Bezuidenhout<sup>\*b</sup>

<sup>a</sup> *Chemistry Department, University of Pretoria, Private Bag X20, Hatfield 0028, Pretoria, South Africa*

<sup>b</sup> *Laboratory of Inorganic Chemistry, Environmental and Chemical Engineering, University of Oulu, P. O. Box 3000, 90014 Oulu, Finland*

\*Email: daniela.bezuidenhout@oulu.fi

#### Table of contents

S1.	Precursor NMR data	S2
S2.	Synthesis of complexes	S2
S3.	2D-NMR Spectroscopy	S3
S4.	Single crystal X-ray diffraction	S5
S5.	References	S8

## S1. Precursor NMR data

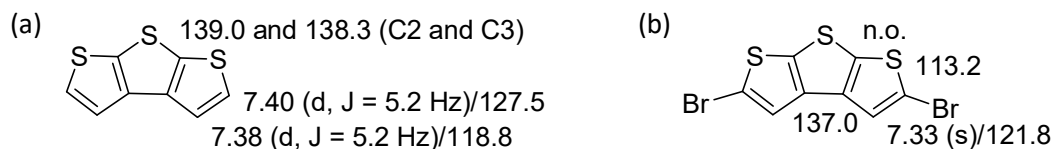


Figure S1.  $^1\text{H}$  /  $^{13}\text{C}$  NMR chemical shifts (ppm) for **P1** (a) and **P2** (b) measured in  $\text{CDCl}_3$

## S2. Synthesis of complexes

Table S1. Yields and colours of complex products obtained from method 1

Compound	Name	Mass (g)	Yield (%)	Colour
Butyl carbene <sup>1</sup>	$[\text{Cr}(\text{CO})_5\{\text{C}(\text{OEt})\text{C}_4\text{H}_9\}]$	0.034	4	Yellow
<b>1</b>	$[\{2\text{-SBu},5\text{-C}(\text{OEt})\text{Cr}(\text{CO})_5\}\text{C}_4\text{HS-3,3}'\text{-C}_4\text{H}_3\text{S}]$	0.29	32	Red
<b>2</b>	$[2'\text{-SBu-C}_4\text{H}_2\text{S-3,3}'\text{-}\{2\text{-C}(\text{OEt})\text{Cr}(\text{CO})_5\}\text{C}_4\text{H}_2\text{S}]$	0.070	8	Yellow-orange
<b>3</b>	$[\{2\text{-SBu},5\text{-C}(\text{OEt})\text{Cr}(\text{CO})_5\}\text{C}_4\text{HS-3,3}'\text{-}\{2'\text{-C}(\text{OEt})\text{Cr}(\text{CO})_5\}\text{C}_4\text{H}_2\text{S}]$	0.32	24	Red-purple
<b>4</b>	$[\{2\text{-SBu},5\text{-C}(\text{OEt})\text{Cr}(\text{CO})_5\}\text{C}_4\text{HS-3,3}'\text{-}\{5'\text{-C}(\text{OEt})\text{Cr}(\text{CO})_5\}\text{C}_4\text{H}_2\text{S}]$		< 3	Red-purple

Table S2. Yields and colours of complex products obtained from method 2

Compound	Name	Mass (g)	Yield (%)	Colour
<b>P1</b>	$\text{C}_8\text{H}_4\text{S}_3$	0.17	47	White
<b>6</b> <sup>2</sup>	$[\text{Cr}(\text{CO})_5\{\text{CNET}\}]$	0.032	4	White
<b>7</b>	$[\text{Cr}(\text{CO})_4\{\text{C}(\text{OEt})\text{-5-C}_8\text{H}_3\text{S}_3\}\text{CNET}]$	0.10	12	Purple-pink

Table S3. Yields and colours of complex products obtained from method 3

Compound	Name	Mass (g)	Yield (%)	Colour
<b>8</b> <sup>3</sup>	$[\{5\text{-C}(\text{OEt})\text{Cr}(\text{CO})_5\}\text{C}_4\text{H}_2\text{S}\text{-3,3}'\text{-C}_4\text{H}_3\text{S}]$	0.14	21	Red
<b>9</b> <sup>3</sup>	$[5,5'\text{-}\{\text{Cr}(\text{CO})_5\text{C}(\text{OEt})\}_2\text{-3,3}'\text{-C}_8\text{H}_4\text{S}_2]$	0.37	35	Purple-red

Table S4. Yields and colours of complex products obtained from method 4

Compound	Name	Mass (g)	Yield (%)	Colour
<b>10</b>	$[\text{Cr}(\text{CO})_5\{\text{C}(\text{OEt})\text{-5-C}_8\text{H}_3\text{S}_3\}]$	0.084	44	Red-orange
<b>1</b>	$[\{2\text{-SBu},5\text{-C}(\text{OEt})\text{Cr}(\text{CO})_5\}\text{C}_4\text{HS-3,3}'\text{-C}_4\text{H}_3\text{S}]$	0.010	5	Red
<b>5</b>	$[\{\text{Cr}(\text{CO})_5\text{C}(\text{OEt})\}_2\text{-5,5}'\text{-C}_8\text{H}_2\text{S}_3]$		< 3	Purple-red

Table S5. Yields and colours of complex products obtained from method 4

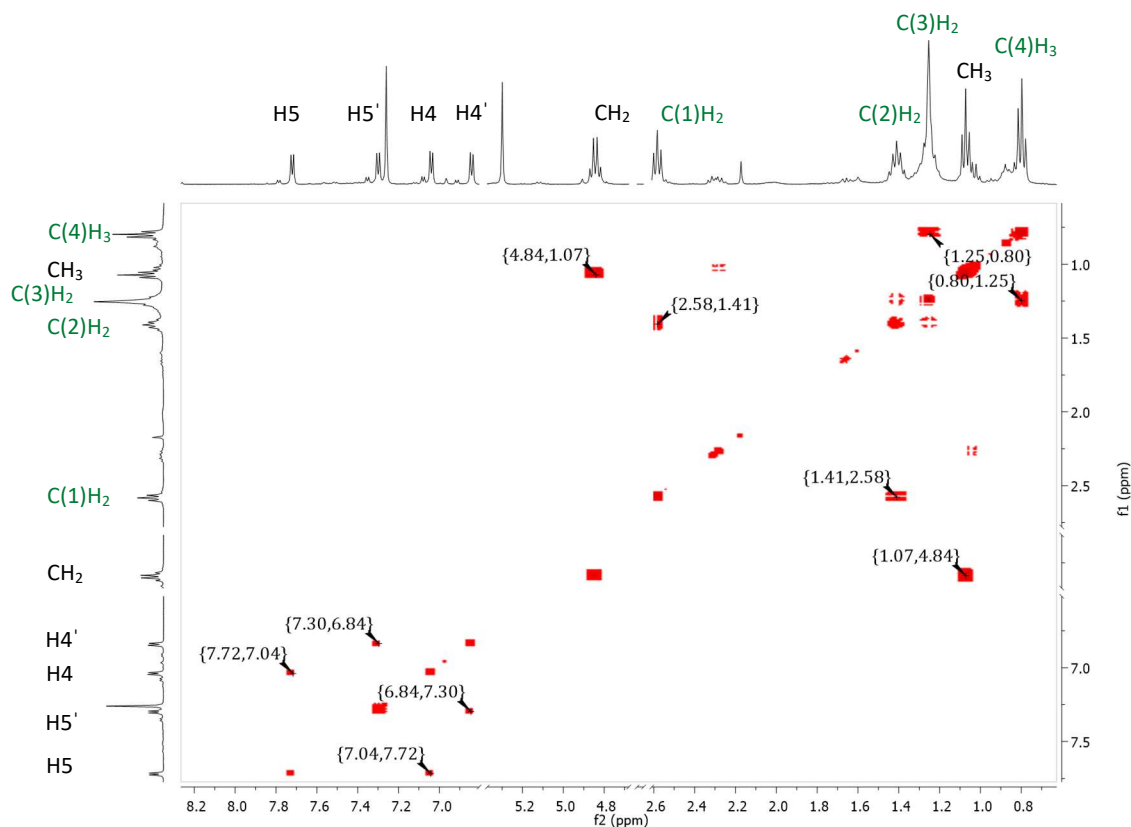
Compound	Name	Mass (g)	Yield (%)	Colour
<b>P1</b>	$\text{C}_8\text{H}_4\text{S}_3$	0.12	20	White
<b>11</b>	$[\text{W}(\text{CO})_5\{\text{C}(\text{OEt})\text{-5-C}_8\text{H}_3\text{S}_3\}]$	0.62	36	Red-orange

**Table S6.** Yields and colours of complex products obtained from method 5

Compound	Name	Mass (g)	Yield (%)	Colour
<b>P1</b>	C <sub>8</sub> H <sub>4</sub> S <sub>3</sub>	0.035	8	White
<b>12</b>	[W(CO) <sub>5</sub> C(NMe <sub>2</sub> )-5-C <sub>8</sub> H <sub>3</sub> S <sub>3</sub> ]	0.44	69	Yellow
<b>13</b>	[{W(CO) <sub>5</sub> C(NMe <sub>2</sub> ) <sub>2</sub> -5,5'-C <sub>8</sub> H <sub>2</sub> S <sub>3</sub> }]	0.22	21	Yellow orange

### S3. 2D NMR spectroscopy

Assignments of proton resonances are made by taking into account the coupling constants of the proton chemical shifts. Challenging proton and carbon assignments are resolved using 2D NMR spectra. The homonuclear chemical shift correlation (<sup>1</sup>H, <sup>1</sup>H) COSY) NMR spectrum is essential in the case of **2** to confirm which aromatic proton doublets (four with similar coupling constants) are coupled. The sequence of proton resonances for the SBU fragment could also be determined with a [<sup>1</sup>H, <sup>1</sup>H] COSY NMR spectrum and is labelled as SC(1)H<sub>2</sub>C(2)H<sub>2</sub>C(3)H<sub>2</sub>C(4)H<sub>3</sub> (green, Fig. S2).

**Figure S2.** 2D [<sup>1</sup>H, <sup>1</sup>H] COSY spectrum of **2**

The [<sup>1</sup>H, <sup>13</sup>C] HSQC NMR spectrum (Fig. S3) is used to assign the protonated carbons of **2**. Quaternary carbons are determined by making use of the heteronuclear multiple bond correlation (<sup>1</sup>H, <sup>13</sup>C) HMBC) NMR spectrum (Fig. S4).

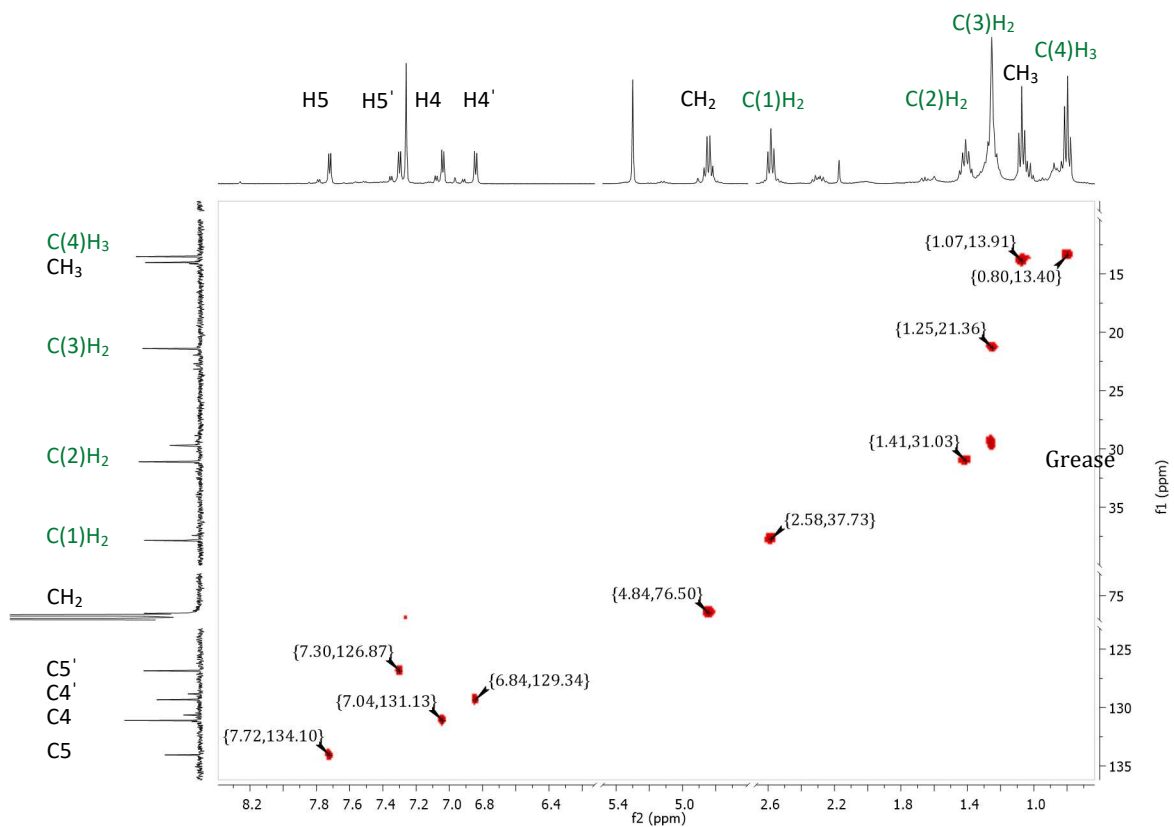


Figure S3. 2D  $^1\text{H}$ ,  $^{13}\text{C}$  HSQC spectrum of **2**

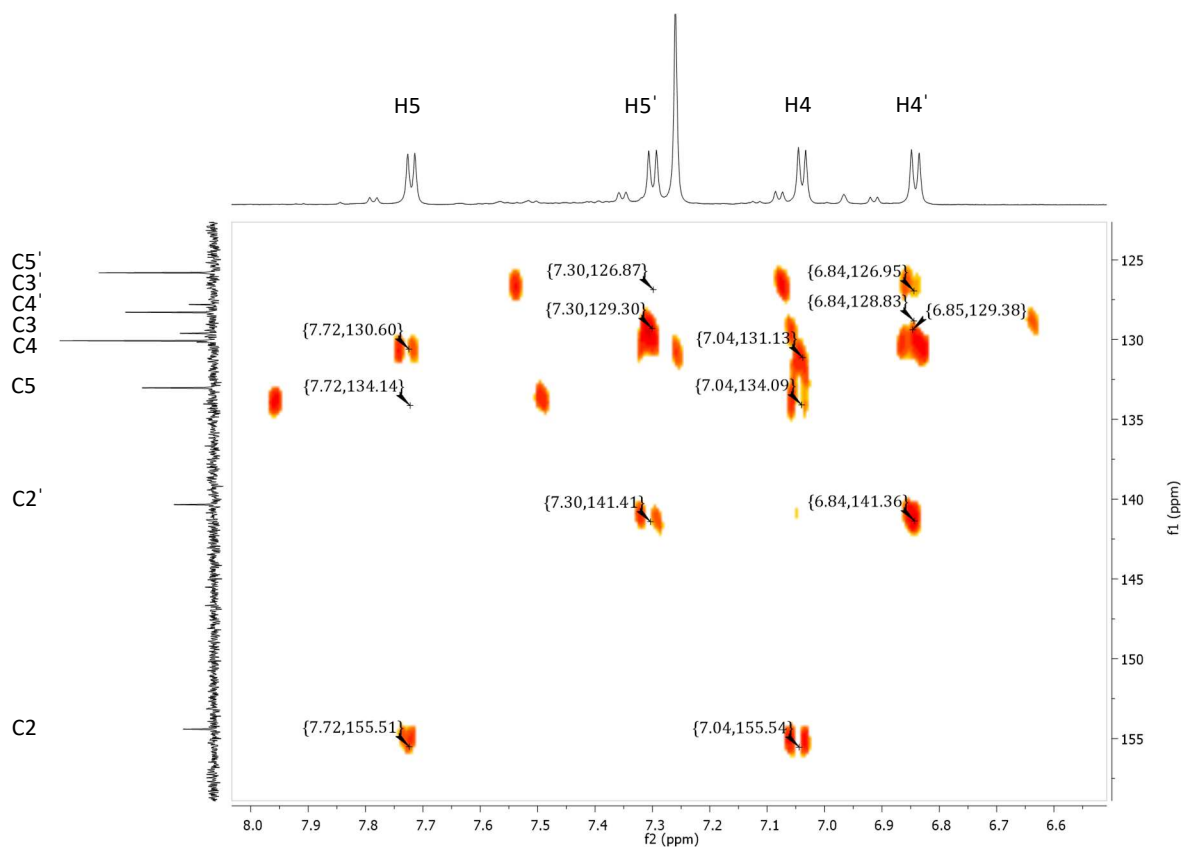
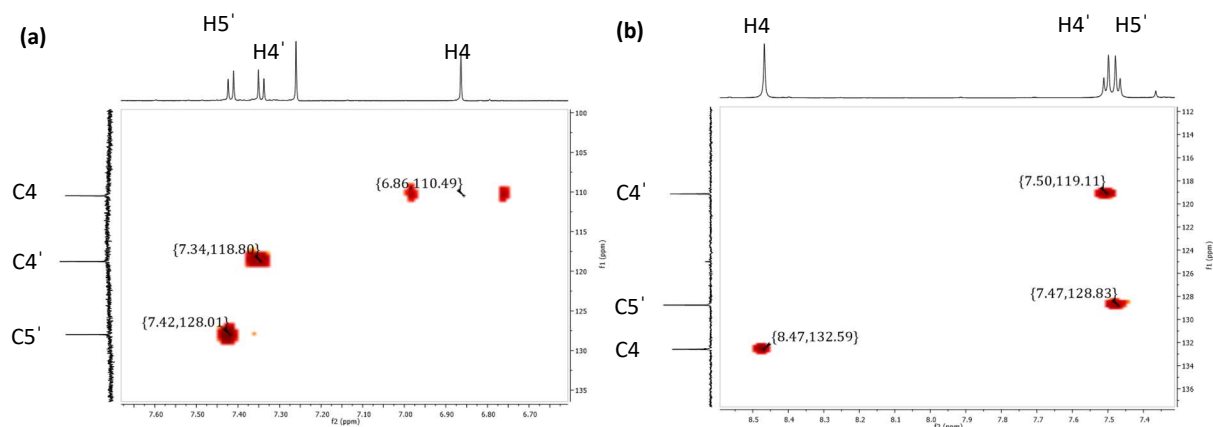


Figure S4. 2D  $^1\text{H}$ ,  $^{13}\text{C}$  HMBC spectrum of **2**

Most thienylene carbene compounds show the H5' resonance more downfield compared to H4' in the  $^1\text{H}$  NMR spectrum (Table 1 and Fig. S5(a)). Compounds **10** (Fig. S5(b)) and **11** are exceptions to this, with their H4' resonances more downfield.



**Figure S5.** 2D [ $^1\text{H}$ ,  $^{13}\text{C}$ ] HSQC spectra of **12** (a) and **10** (b), showing only the aromatic regions

## S4 Single crystal X-ray diffraction

### S4.1 Crystal data collection and structure refinement parameters

**Compound 1:**  $\text{C}_{20}\text{H}_{18}\text{O}_6\text{S}_3\text{Cr}$  ( $M = 502.56$  g/mol): monoclinic, space group  $C2/c$  (no. 15),  $a = 52.4504(19)$  Å,  $b = 7.4685(3)$  Å,  $c = 25.3205(9)$  Å,  $\beta = 114.7700(10)^\circ$ ,  $V = 9006.1(6)$  Å<sup>3</sup>,  $Z = 16$ ,  $T = 150.01$  K,  $\mu(\text{Mo K}\alpha) = 0.819$  mm<sup>-1</sup>,  $D_{\text{calc}} = 1.4825$  g/cm<sup>3</sup>, 156088 reflections measured ( $4.54^\circ \leq 2\theta \leq 49.42^\circ$ ), 7672 unique ( $R_{\text{int}} = 0.0424$ ,  $R_{\text{sigma}} = 0.0230$ ) which were used in all calculations. The final  $R_1$  was 0.0325 ( $I > 2\sigma(I)$ ) and  $wR_2$  was 0.1008 (all data). CCDC 2009044

**Compound 5:**  $\text{C}_{24}\text{H}_{12}\text{Cr}_2\text{O}_{12}\text{S}_3$  ( $M = 692.52$  g/mol): triclinic, space group  $P-1$  (no. 2),  $a = 7.7699(7)$  Å,  $b = 10.8891(11)$  Å,  $c = 17.2416(17)$  Å,  $\alpha = 104.632(4)^\circ$ ,  $\beta = 94.044(4)^\circ$ ,  $\gamma = 96.766(4)^\circ$ ,  $V = 1394.0(2)$  Å<sup>3</sup>,  $Z = 2$ ,  $T = 150(2)$  K,  $\mu(\text{MoK}\alpha) = 1.066$  mm<sup>-1</sup>,  $D_{\text{calc}} = 1.650$  g/cm<sup>3</sup>, 31826 reflections measured ( $4.91^\circ \leq 2\theta \leq 49.424^\circ$ ), 4749 unique ( $R_{\text{int}} = 0.1147$ ,  $R_{\text{sigma}} = 0.0626$ ) which were used in all calculations. The final  $R_1$  was 0.0309 ( $I > 2\sigma(I)$ ) and  $wR_2$  was 0.0830 (all data). CCDC 2009043

**Compound 7:**  $\text{C}_9\text{H}_{6.5}\text{Cr}_{0.5}\text{N}_{0.5}\text{O}_{2.5}\text{S}_{1.5}$  ( $M = 235.74$  g/mol): triclinic, space group  $P-1$  (no. 2),  $a = 7.4794(7)$  Å,  $b = 11.9763(11)$  Å,  $c = 12.1963(12)$  Å,  $\alpha = 110.742(3)^\circ$ ,  $\beta = 91.017(3)^\circ$ ,  $\gamma = 103.342(3)^\circ$ ,  $V = 988.15(16)$  Å<sup>3</sup>,  $Z = 4$ ,  $T = 150(2)$  K,  $\mu(\text{MoK}\alpha) = 0.926$  mm<sup>-1</sup>,  $D_{\text{calc}} = 1.585$  g/cm<sup>3</sup>, 28214 reflections measured ( $5.632^\circ \leq 2\theta \leq 52.044^\circ$ ), 3883 unique ( $R_{\text{int}} = 0.0336$ ,  $R_{\text{sigma}} = 0.0199$ ) which were used in all calculations. The final  $R_1$  was 0.0285 ( $I > 2\sigma(I)$ ) and  $wR_2$  was 0.0722 (all data). CCDC 2009042

**Compound 10:**  $C_{16}H_8CrO_6S_3$  ( $M = 444.40$  g/mol): triclinic, space group P-1 (no. 2),  $a = 6.8382(7)$  Å,  $b = 9.8055(10)$  Å,  $c = 14.0893(13)$  Å,  $\alpha = 104.167(3)^\circ$ ,  $\beta = 97.269(3)^\circ$ ,  $\gamma = 104.205(3)^\circ$ ,  $V = 870.30(15)$  Å<sup>3</sup>,  $Z = 2$ ,  $T = 150(2)$  K,  $\mu(\text{MoK}\alpha) = 1.048$  mm<sup>-1</sup>,  $D_{\text{calc}} = 1.696$  g/cm<sup>3</sup>, 20020 reflections measured ( $4.472^\circ \leq 2\theta \leq 49.424^\circ$ ), 2957 unique ( $R_{\text{int}} = 0.0354$ ,  $R_{\text{sigma}} = 0.0224$ ) which were used in all calculations. The final  $R_1$  was 0.0280 ( $I > 2\sigma(I)$ ) and  $wR_2$  was 0.0692 (all data). CCDC 2009045

**Compound 11:**  $C_{19}H_8O_9S_3W_{1.5}$  ( $M = 752.23$  g/mol): triclinic, space group P-1 (no. 2),  $a = 7.64250(10)$  Å,  $b = 9.4015(2)$  Å,  $c = 16.0890(3)$  Å,  $\alpha = 94.7090(10)^\circ$ ,  $\beta = 99.6690(10)^\circ$ ,  $\gamma = 90.3600(10)^\circ$ ,  $V = 1135.50(4)$  Å<sup>3</sup>,  $Z = 2$ ,  $T = \text{N/A}$  K,  $\mu(\text{Cu K}\alpha) = 16.960$  mm<sup>-1</sup>,  $D_{\text{calc}} = 2.2000$  g/cm<sup>3</sup>, 23355 reflections measured ( $5.6^\circ \leq 2\theta \leq 144.24^\circ$ ), 4461 unique ( $R_{\text{int}} = 0.0897$ ,  $R_{\text{sigma}} = 0.0597$ ) which were used in all calculations. The final  $R_1$  was 0.0489 ( $I \geq 2\sigma(I)$ ) and  $wR_2$  was 0.1236 (all data). CCDC 2009041

**Compound 12:**  $C_{16}H_9NO_5S_3W$  ( $M = 572.25$  g/mol): monoclinic, space group  $P2_1/c$  (no. 14),  $a = 19.5378(6)$  Å,  $b = 6.4155(2)$  Å,  $c = 15.0044(4)$  Å,  $\beta = 99.372(3)^\circ$ ,  $V = 1855.62(10)$  Å<sup>3</sup>,  $Z = 4$ ,  $T = 150(2)$  K,  $\mu(\text{MoK}\alpha) = 6.589$  mm<sup>-1</sup>,  $D_{\text{calc}} = 2.048$  g/cm<sup>3</sup>, 20159 reflections measured ( $4.226^\circ \leq 2\theta \leq 52.74^\circ$ ), 3788 unique ( $R_{\text{int}} = 0.1421$ ,  $R_{\text{sigma}} = 0.0541$ ) which were used in all calculations. The final  $R_1$  was 0.0528 ( $I > 2\sigma(I)$ ) and  $wR_2$  was 0.1438 (all data). CCDC 2009047

**Compound 13:**  $C_{24}H_{14}N_2O_{10}S_3W_2$  ( $M = 954.25$  g/mol): monoclinic, space group  $P2_1/n$  (no. 14),  $a = 6.5741(5)$  Å,  $b = 15.1714(10)$  Å,  $c = 32.440(2)$  Å,  $\beta = 95.543(3)^\circ$ ,  $V = 3220.4(4)$  Å<sup>3</sup>,  $Z = 4$ ,  $T = 150.15$  K,  $\mu(\text{CuK}\alpha) = 15.285$  mm<sup>-1</sup>,  $D_{\text{calc}} = 1.968$  g/cm<sup>3</sup>, 130982 reflections measured ( $5.474^\circ \leq 2\theta \leq 144.236^\circ$ ), 6328 unique ( $R_{\text{int}} = 0.1304$ ,  $R_{\text{sigma}} = 0.0470$ ) which were used in all calculations. The final  $R_1$  was 0.0582 ( $I > 2\sigma(I)$ ) and  $wR_2$  was 0.2062 (all data). CCDC 2009046

#### S4.2 X-ray crystallography: packing

The molecules do not fit exactly on top of each other in the  $\pi$ - $\pi$  stacking observed for **10** and **11**, but their [2,3-*b*;3',2'-*d*]-DTT spacers overlap (Fig. S6). Classical  $\pi$ - $\pi$  stacking is also observed in **1**, **5** and **7** with their  $\pi$ - $\pi$  interaction distances measured as 3.549, 4.434 and 3.772 Å respectively. Only partial overlap of the thienylene spacers occur.

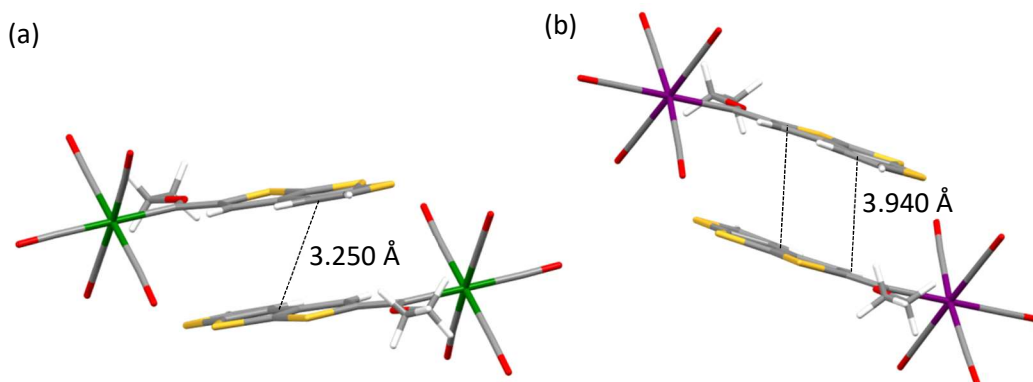


**Figure S6.**  $\pi$ - $\pi$  Stacking of **10** (a) and **11**(b) when viewed down the crystallographic *b*-axis

The packing of **13** shows stacking and columnar packing when viewed down two different axes. This basic structural motif (columns) can be divided into different levels of crystal organization, primary (columns) and secondary (layers of columns). The columns are assigned to columnar packing, consisting of molecules that pack with small  $\pi$ - $\pi$  interaction distances, for example **13**, when viewed down the crystallographic *a*-axis (Fig. S7(a)). The molecules fit on top of each other, down the column, in a parallel fashion. The columns are parallel-packed in a non-planar fashion, with each column surrounded by eight other columns. The  $\pi$ - $\pi$  interaction distance is measured at 6.574 Å, too far apart to be called true  $\pi$ - $\pi$  stacking (3.5-5 Å). Rather, a packing pattern is seen where the units are merely densely packed. The formation of a grid network is evident from the view along the crystallographic *a*-axis, consisting of dimers that are packed antiparallel to each other.

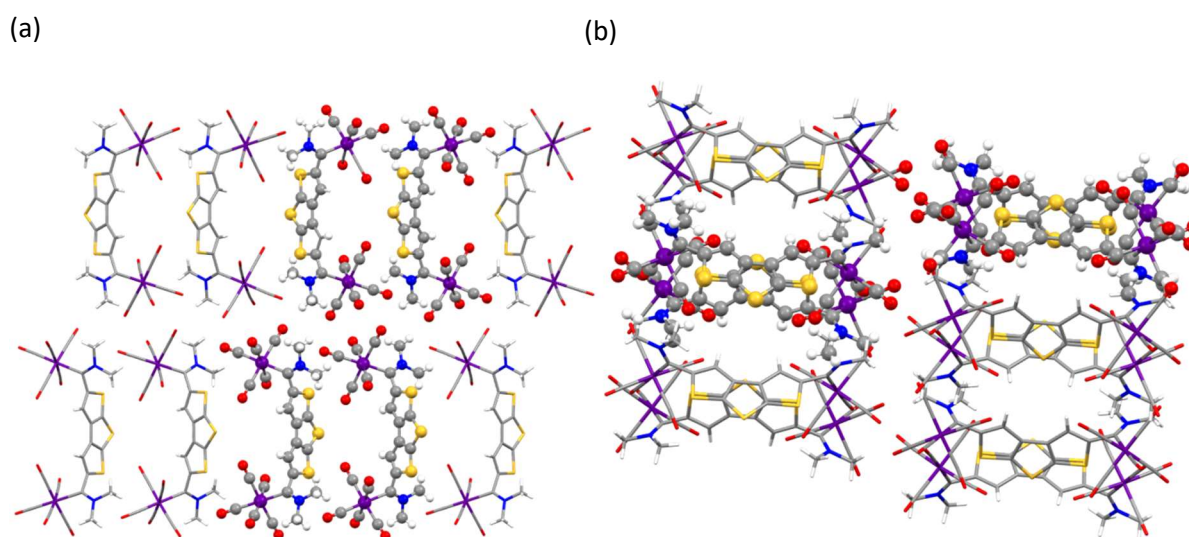


**Figure S7.** Packing of **13** viewed down the crystallographic *a*-axis (a) and *b*-axis (b)

The layers of columns consist of packed molecules with longer  $\pi$ - $\pi$  separation distances, for example **13** has a separation distance of 15.171 Å, when viewed down the crystallographic *b*-axis (Fig. S7(b)). The molecules fit on top of each other, down the column, with the columns packed together in dimers. The dimer columns pack parallel, but steric hindrance prevents them from packing planar to each other, hence they are interlocking.

#### S5 References.

1. Terblans, Y. M.; Marita Roos, H.; Lotz, S. *J. Organomet. Chem.* **1998**, *566*, 133–142.
2. Connor, J. A.; Jones, E. M.; McEwen, G. K.; Lloyd, M. K.; McCleverty, J. A. *J. Chem. Soc., Dalton Trans.* **1972**, No. 12, 1246.
3. Lamprecht, Z.; Moeng, M. M.; Liles, D. C.; Lotz, S.; Bezuidenhout, D. I. *Polyhedron* **2019**, *158*, 193–207.